Polymer 50 (2009) 5490–5498

Contents lists available at ScienceDirect

Polymer

journal homepage: www.elsevier.com/locate/polymer

Kinetics and dynamics of thermally-induced shape-memory behavior of crosslinked short-chain branched polyethylenes

Igor S. Kolesov [a], Karl Kratz [b], Andreas Lendlein [b], Hans-Joachim Radusch [a,*]

[a] Martin Luther University Halle-Wittenberg, Center of Engineering Sciences, D-06099 Halle (Saale), Germany
[b] Institute of Polymer Research, GKSS Research Center, Kant Str. 55, 14513 Teltow, Germany

ARTICLE INFO

Article history:
Received 28 May 2009
Received in revised form
31 August 2009
Accepted 21 September 2009
Available online 26 September 2009

Keywords:
Shape-memory effect
Ethylene-1-octene copolymers
Peroxidic crosslinking

ABSTRACT

Systematic investigation of the relation between shape-memory (SM) behavior and characteristics of the covalent network and the crystalline domains of a crosslinked polymer, i.e., crosslink density and crystallinity, respectively, was performed using homogeneous ethylene-1-octenecopolymers (EOC) as model polymers. The EOCs have been crosslinked by 2,5-dimethyl-2,5-di(t-butylperoxy)hexane (DHBP) decomposition. Two EOCs with a degree of branching of 30 and 60 hexyl side chains per 1000C atoms with each four different crosslink densities were employed. The investigated EOCs differ significantly in crystallinity, melting temperature (T_m) and crosslink density. The crosslinked EOC undergone the programming at a strain of 100% showed high strain fixity ratio (R_f) and strain recovery ratio (R_r). The R_f and R_r values increase with increasing crystallinity and crosslink density, respectively, and decline only slightly in a subsequent SM cycle. The switching temperature (T_{sw}) is strictly related to T_m and decreases with increasing degree of branching as well as crosslink density in the temperature range of 101–63 °C. T_{sw} remains nearly unchanged when the programming temperature (T_{pr}) or the load during SM recovery is varied. The kinetics of SM recovery as characterized by the temperature dependence of recovery rate is controlled by the melting behavior. The specific work generated by the programmed specimen during thermally-induced recovery under constant load, gains with increasing crosslink density, and is proposed as dynamical characteristic of practical relevance. The opportunity of tailoring T_{sw} by variation of the degree of branching and crosslink density makes such polymers attractive candidates for applications requiring T_{sw} temperatures in the range from 60 to 100 °C.

1. Introduction

Shape-memory polymers (SMP) represent a promising class of smart polymers [1–6], which can be advantageously used in various fields of application, e.g., as heat-shrinkable tubing and films, particularly in electrical cables, packaging [7,8] and automotive industry [3,4]. SMP are also being developed for biomedical applications, e.g., such as stents and microtubing for therapeutic actuators, and suture materials [9–14]. For such applications only biocompatible polymers come into consideration [1–4,9–16]. In many cases the SMP needs to be biodegradable as well [9,12,17–20].

Preconditions for proper observation of the thermally-induced SM effect (SME) are the existence of a covalently crosslinked or a stable physically network, as well as a thermal transition (e.g., melting) at convenient temperatures T_{trans} [1]. For covalently crosslinked semi-crystalline polymers, e.g., if crosslinking is realized by peroxide decomposition, a SM behavior with high performance can be achieved, if the following requirements are fulfilled. Firstly, the polymeric material must possess a thermally and mechanically resistant network with suitable high crosslink density in order to produce sufficiently large elastic and viscoelastic forces under load at programming temperature $T_{pr} > T_{trans}$ and preferably minimal residual strain. Also, a sufficient elongation at break of the material is necessary. Secondly, the crystalline phase formed after cooling of the stretched sample must be able to fix the strain and the elastic/viscoelastic forces stored in the network. The ability of SMP to fix a temporary shape and to restore a permanent (original) shape are characterized by the strain fixity ratio (R_f) and strain recovery ratio (R_r), which are defined according to [1] as:

$$R_f = \frac{\varepsilon_{rem}}{\varepsilon_{pr}} \quad \text{and} \quad R_r = \frac{\varepsilon_{pr} - \varepsilon_{rec,m}}{\varepsilon_{pr}} \tag{1}$$

* Corresponding author. Tel.: +49 0 3461 46 2590; fax: +49 0 3461 46 3891.
E-mail address: hans-joachim.radusch@iw.uni-halle.de (H.-J. Radusch).

0032-3861/$ – see front matter © 2009 Elsevier Ltd. All rights reserved.
doi:10.1016/j.polymer.2009.09.062

where ε_{pr} is the programming strain, i.e. strain produced by stretching during programming, ε_{rem} is the remaining strain after completed programming, i.e. after cooling to the lowest temperature of experiment, unloading and recovery of the stretched specimen at room temperature, and $\varepsilon_{rec,m}$ is the residual strain measured as thermally-induced recovery (shrinkage) at maximum temperature of experiment. In the case of ideal SM behavior the relations $\varepsilon_{rem} = \varepsilon_{pr}$ and $\varepsilon_{rec,m} = 0$ are valid.

If strain recovery is recorded at constant heating rate, the relation between temperature and measuring time is linear. In this connection the kinetics of SM recovery can be described by means of the recovery rate, i.e. the first derivative of recovery strain ($\varepsilon_{rec}(T)/dt$) with respect to the time ($d\varepsilon_{rec}(T)/dt$). For characterization of the SM recovery kinetics the absolute peak value of recovery rate $|d\varepsilon_{rec}(T)/dt|_{max}$ has been employed. The switching temperature (T_{sw}), as a further important characteristic of SME, was estimated as the temperature, which corresponds to the peak of recovery rate, in contrast to the other definitions of T_{sw}, as for example a temperature calculated by the equation $\varepsilon_{rec}(T_{sw})\cdot 100\% = 0.5\ R_r$ [21,22].

Unfortunately, in many publications [2–22] on the dynamical aspects of SME in polymers has not been reported. Therefore, a series of excellent works performed in both three-point bending [23–25] as well as uniaxial tension and compression modes [26,27] should be especially emphasized. Both the thermally-induced recovery and the release of stored stress under various external constrains of SMP programmed at a strain of about 10% at different temperatures were investigated experimentally and theoretically analyzed on the basis of a developed constitutive model [23–27]. An important finding is in particular the observation that the SM recovery under load and the corresponding effective values of R_r decrease considerably with increasing constraining stress σ_{rec} and approach to zero, if σ_{rec} reaches the programming stress σ_{pr} [24,25]. However, it should be noted that firstly the last result was demonstrated only in tree-point bending mode and secondly all the detected results are obtained only for relatively low strain and only for SMP with glass transition as switching mechanism [23–27]. In the present work the dynamics of SM behavior is evaluated on the basis of SM recovery under load by constant external opposed force using the relatively high programming strain of 100% and by means of short-term stress relaxation at T_{pr}.

The recently published results about SME in ethylene copolymers [21,22] and in polycyclooctene [28] crosslinked by means of dicumyl peroxide (DCP) demonstrate the potential of these types of material for technical applications in comparison to crosslinked conventional polyethylenes (PEs). Moreover, the commercially available homogeneous ethylene-1-octene copolymers (EOC) are suitable model polymers for the study of the mechanisms of thermally-induced SME in crosslinked semi-crystalline polymers due to the possibility for adjusting the temperature range of melting as well as the ability to crystallization and crosslinking by means of the variation of comonomer content [29]. As a matter of fact the investigated EOCs are short-chain branched polyethylenes (SCBPEs) with the random intrinsic homogeneous distribution of short-chain branches or in other words of tertiary carbon atoms along the main chains. The crystallinity, melting and crystallization temperature of SCBPEs decrease with increasing degree of branching due to the shortening of crystallizable ethylene sequences between neighboring tertiary carbon atoms, as already reported for EOC [29]. The experimental results also showed that hydrogen atoms on tertiary carbon atoms are much more easily abstracted than hydrogen atoms attached to secondary and primary carbon atoms [30,31]. These results are in agreement with theoretical calculations [32]. According to [33] the crosslinkability of SCBPEs increases with increasing degree of branching in the range between approximately 16 and 31 CH_3/1000C. Tertiary radicals can also initiate the undesired scission reaction appearing in SCBPEs [34]. However, the contribution of scission reaction prevails only at high degree of branching ($\geq$31 CH_3/1000C) and high peroxide concentration, e.g., at dicumyl peroxide $\geq$ 4 wt% [33].

For the depicted reasons, the objectives of the present work are the systematic investigation of the correlation between the SM behavior of EOCs crosslinked by means of peroxide, on the one hand, and the characteristics of network and crystalline phase as well as SM programming and measuring conditions, on the other hand. The study focuses on the description of basic mechanisms of the thermally-induced SME in crosslinked semi-crystalline polymers and in particular, on the kinetics and dynamics of SM recovery. From the point of view of application as SMP, the important advantage of crosslinked EOCs/SCBPEs compared to crosslinked conventional PEs is the relatively low melting temperature, which even can be only 60 °C depending on the degree of branching and crosslink density. This allows to expect also low T_{sw} values at which the thermally-induced SME can be activated by simple procedures such as heating in hot water.

2. Experimental

2.1. Materials and processing

The SCBPEs used in the present study are commercially available homogeneous EOCs (*Dow Chemical*) produced using metallocene catalysts with approx. 30 and 60 hexyl branches per 1000C (EOC30 and EOC60, respectively). The relevant parameters of these materials are compiled in Table 1. As crosslinking agent 2,5-dimethyl-2,5-di(t-butylperoxy)hexane (DHBP) was employed. The use of DHBP resulted in a higher efficiency and a good processability of the chosen systems compared to DCP due to the availability of two peroxy groups and the higher thermal stability (up to 145 °C) as well as fluidity at room temperature. Pellets of the processed polymers were impregnated with DHBP via mechanical mixing in a hermetic closed plastics flask and diffusion of the peroxide into the polymer pellets for three days at room temperature. For sample preparation the impregnated EOC30 and EOC60 pellets containing the nominal DHBP concentration of 1, 2, 3 and 4 wt% were used. Subsequently, the DHBP containing polymers were homogenized using a single-screw mixing extruder (*Brabender*) at 130 °C barrel temperature. The true DHBP content determined by thermogravimetric analysis (TGA, *Mettler–Toledo*), as given in Table 2, was lower compared to the desired values in all samples. Thereby, the differences between true and desired values increase significantly with increasing crystallinity of the polymer.

The processing experiments show that the applied crosslinking method is suitable for PEs with the chosen melt-flow index MFI (see Table 1) measured by means of the melt index test apparatus MI 21,6 (*Göttfert*). DHBP as a low-molecular fluid substance can act as a lubricant during processing, i.e., the effective MFI values of DHBP-impregnated PEs are evidently higher and the viscosities are lower than that of pure materials. Thus, the DHBP can conduce to the mixing process at 130 °C. The extrudates were compression molded to films with a thickness of 0.5, 1 and 2 mm and crosslinked at a temperature of 190 °C in the press under load. The chosen crosslinking temperature and crosslinking duration were optimized on the basis of time dependency of torque measured using a vulcameter 'Elastograph' (*Göttfert*) at four different temperatures of 170, 180, 190 and 200 °C.

2.2. Network characterization

The crosslink density, which reflects the density of network chains, is connected with $\overline{M}_c$ and the material density ρ at

Table 1
Designations as well as physical and molecular parameters of the used EOCs.

Designation	Melt-flow index [dg/min]			Melting temperature T_m [°C]	Density [kg/m^3]	Mass-average molecular mass $\overline{M}_w$ [kg/mol]	Poly dispersity $\overline{M}_w/\overline{M}_n$ [-]
	190 °C/2.16 kg	190 °C/5.0 kg	130 °C/5.0 kg				
EOC30	5.0	17.7	4.2	96	900	64	2.3
EOC60	4.4	15.9	3.4	59	870	87	2.5

measurement temperature through the simple equation $\nu_c = \overline{M}_c/\rho$. The average molecular mass of the links, i.e., the network chains between two neighboring network nodes $\overline{M}_c$ of EOC crosslinked using different DHBP amounts were calculated by means of the *Flory–Rehner* equation [35] on the basis of swelling measurements. The swelling measurements were performed at the samples stored in xylene at 110 °C after at least 10 h using the gel of crosslinked EOC obtained after extraction of the soluble fraction as described in [33,36]. The extraction experiments were carried out in a *Soxhlet* extractor in xylene at 110 °C for at least 28 h using about 0.7 g samples partitioned into 65 pieces. The ν_c and $\overline{M}_c$ values for both crosslinked EOCs were also evaluated from stress-strain diagrams ascertained at 120 °C on the basis of the *Mooney–Rivlin* equation [37,38]. The results determined for crosslinked EOCs using the both abovementioned methods are in satisfactory agreement with each other (see Table 2). The difference between the results of both used methods is within the experimental error range of 10–20%, which becomes wider with declining ν_c. Hence, in the text, tables and legends below, the mean ν_c values calculated on the basis of both swelling and tensile tests are given. Interestingly, the same quantities of DHBP cause a more close-meshed network in EOC30 compared to EOC60, i.e. the efficiency of crosslinking agent in SCBPEs with high degree of branching is lower, presumably because of an increasing contribution of the scission reaction initiated simultaneously with the crosslinking [33].

However, it has to be also taken into account that the relatively homogenous distribution of network nodes may be expected only in highly branched and correspondingly low crystalline PEs whose very small crystallites, e.g., fringed micelles [29], are dispersed in the continuous and quasi homogenous amorphous phase. The peroxide distribution in medium and high crystalline PEs homogenized in the extruder is definitely no more homogeneous at molecular level after subsequent cooling of the extrudates due to reallocation of the peroxide caused by crystallization. By definition, the originated crystalline regions are free from peroxide. In this connection by reheating until 190 °C these nano-regions obviously will not be crosslinked, and retain the ability to crystallization. Hence, the experimentally acquired average values of crosslink density are definitely considerably lower than the true local crosslink density of the amorphous phase.

The elongation at break values received from tensile tests point to the possibility of using a standard programming strain ε_{pr} of 100% for the investigation of the SM behavior of used materials.

2.3. Instrumentation

Tensile tests in the temperature range of SM tests programming at 120 °C has been carried out using a testing machine Zwick 1425 (*Zwick*) with heating chamber and a load cell 10 N at a cross head speed of 5 mm/min after DIN EN ISO 527-1. As specimens, shouldered test bars with the cross-section area 2.0×2.0 mm^2 were used. The initial distance between the clamps was 21 mm.

Thermal analysis of crosslinked EOC30 and EOC60 was performed with DSC-7 (*Perkin–Elmer*) at a heating rate of 20 K/min. The experimental data were converted into temperature dependencies of apparently heat capacity $c_p(T)$ as described earlier [39,40]. The measured $c_p(T)$ values in conjunction with theoretical $c_p(T)$ values for crystalline and amorphous PE were utilized for the calculation of an enthalpy-based crystallinity as proposed in [41].

SM behavior investigations were carried out in tensile mode using a mechanical spectrometer measuring head Mark III (*Rheometric Scientific*). The samples shaped as strips with a cross-section area 2.0×1.0 mm^2 were tested during the specific cyclic thermo–mechanical experiment at an initial clamps distance of 12 mm. The samples were programmed by a tensile strain of $\varepsilon_{pr} = 100\%$ during a standard dwell period of 120 s at the T_{pr}, and cooled down to the lowest temperature T_{low} of 10 or 0 °C for EOC30 and EOC60, respectively, in the constant deformed state at an average cooling rate of 11 K/min. The values of programming stress σ_{pr} were measured at T_{pr} for 120 s after loading of the sample. The stretched specimen was thermally equilibrated for 10 min at T_{low}, unloaded and heated to 25 °C. After a dwell time of 10 min at 25 °C the remaining strain ε_{rem} for estimation of R_f was determined, and than the unconstrained thermally-induced recovery of the completely programmed sample in a heating run at a rate of 2 K/min and 'zero' stress of 70 Pa was measured. In order to estimate the 'fatigue' of SM polymer the described cycle was additionally repeated two times for each specimen. The effect of load on the specific work, generated by the programmed specimen during SM recovery was investigated under constraining stress σ_{rec} of 0.1 and 0.2 MPa. Because of the unconventional nature of this kind of experiment, the experimental details are discussed together with the results in Section 3.3.

3. Results and discussion

3.1. Melting behavior and crystallinity

Fig. 1 shows the enthalpy-based crystallinity versus temperature obtained in first heating runs for both uncrosslinked and cured

Table 2
Crosslink density ν_c and average molecular mass of link $\overline{M}_c$ of medium branched EOC30 and highly branched EOC60 estimated on the basis of tensile and swelling tests depending on DHBP content.

EOC30					EOC60				
DHBP content [wt%]	ν_c [mol m^{-3}]		$\overline{M}_c$ [kg/mol]		DHBP content [wt%]	ν_c [mol m^{-3}]		$\overline{M}_c$ [kg/mol]	
	Tens. Test	Swell. Test	Tens. Test	Swell. Test		Tens. Test	Swell. Test	Tens. Test	Swell. Test
0.5	56	75	14.39	10.37	0.9	38	63	21.21	11.54
1.1	142	134	5.68	6.02	1.9	105	126	7.68	6.40
1.6	213	224	3.78	3.60	2.7	151	149	5.34	5.43
1.9	274	264	2.94	3.05	3.6	192	193	4.20	4.17

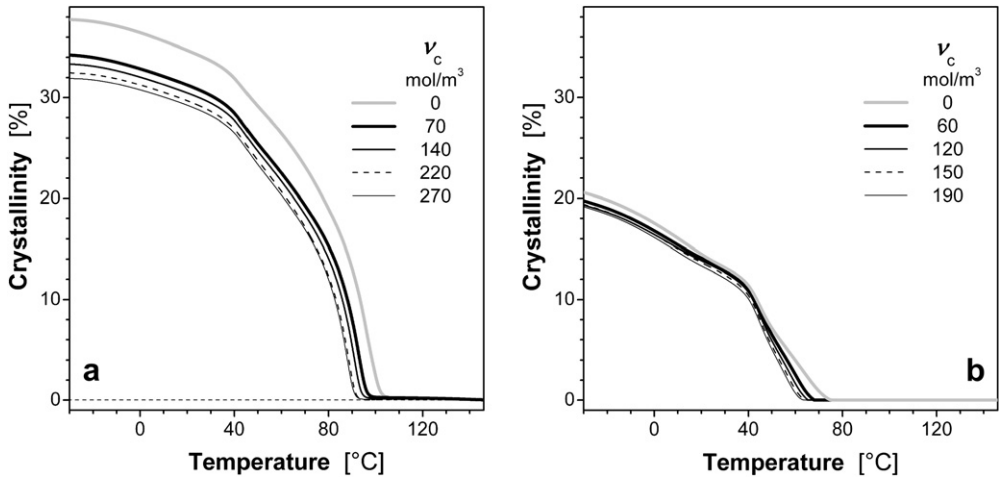

Fig. 1. Enthalpy-based crystallinity versus temperature obtained for medium branched EOC30 (a) and highly branched EOC60 (b) depending on the crosslink density ν_c.

EOC30 and EOC60. Both highly branched EOC60 and medium branched EOC30 exhibit the fragmentation of the c_p melting peak which results in the discontinuity of crystallinity as function of temperature. This phenomenon is caused by annealing at room temperature during storage of prepared samples. The second crystal population generated by annealing has a poorer quality and subsequently lower thermal stability as it was shown for uncrosslinked EOCs especially with high branch degree [42].

The consistent decrease of the final melting temperature T_m and the crystallinity in the entire temperature range takes place with increasing crosslink density for both EOC30 (from 96 to 88 °C and from 35 to 29% at 25 °C, respectively) and EOC60 (from 64 to 56 °C and from 14 to 13% at 25 °C, respectively). The decrease of crystallinity for medium branched EOC30 is more distinct than that of highly branched EOC60. The depicted reduction of T_m values with increasing crosslink density reflects obviously the reduction of perfection and size of crystallites in particular the decrease of lamellae thickness.

3.2. Effect of degree of branching and crosslink density, programming temperature and cyclic thermo–mechanical load on unconstrained SM behavior of EOCs

Fig. 2 depicts the influence of crosslinking degree of medium EOC30 (a, b) and highly branched EOC60 (c, d) on the conventional characteristics and kinetics of thermally-induced SM recovery in

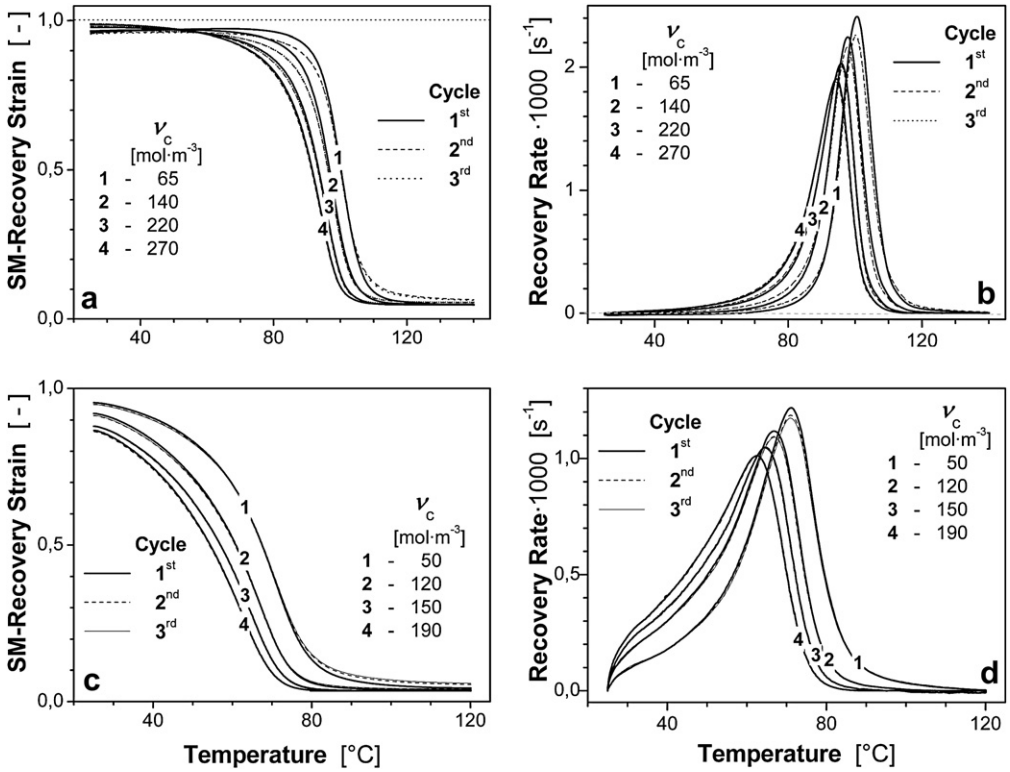

Fig. 2. Temperature dependencies of SM recovery strain (a, c) and recovery strain rate (b, d) measured in three repeating thermo–mechanical load-recovery cycles for EOC30 (a, b) and EOC60 (c, d) with four different crosslink density ν_c after programming at 100 and 80 °C, respectively.

Table 3
Influence of crosslink density ν_c, programming temperature T_{pr} and cyclic thermo–mechanical load on programming stress σ_{pr} and SME characteristics of medium and highly branched EOC.

EOC type	ν_c [mol m^{-3}]	T_m [°C]	T_{pr} [°C]	Cycle #	σ_{pr} [MPa]	R_f [%]	R_r [%]	T_{sw} [°C]	$\lvert d\varepsilon_{rec}(T)/dt\rvert_{max}$ [10^{-3} s^{-1}]
EOC30	65	93.1	100	1st	0.97	96.0	95.2	100.6	2.41
				2nd	0.93	95.6	93.7	100.2	2.25
				3rd	0.91	95.5	93.5	100.2	2.26
	140	91.0	100	1st	1.45	96.5	95.0	97.8	2.24
				2nd	1.41	96.5	94.5	97.7	2.17
				3rd	1.42	96.5	94.3	97.7	2.17
			120	1st	1.51	96.6	95.3	98.2	2.23
			140	1st	1.65	97.1	93.4	98.3	2.16
				2nd	1.45	97.2	90.2	98.2	2.11
				3rd	1.56	97.2	87.7	98.2	2.07
	220	89.0	100	1st	1.85	97.7	95.2	95.9	2.03
				2nd	1.84	98.1	95.0	95.9	2.01
				3rd	1.84	98.1	94.9	95.9	2.00
	270	88.2	100	1st	2.05	98.6	95.0	94.5	1.90
				2nd	2.05	99.0	94.9	94.4	1.88
				3rd	2.04	99.0	94.9	94.4	1.88
EOC60	50	60.2	80	1st	0.60	95.5	95.7	71.2	1.22
				2nd	0.58	95.0	94.5	71.0	1.19
				3rd	0.57	94.9	94.2	71.1	1.17
			120	1st	0.56	94.7	93.4	71.4	1.12
				2nd	0.54	95.0	92.2	71.3	1.10
				3rd	0.53	95.0	91.6	71.2	1.09
	120	57.9	80	1st	0.943	92.1	96.3	66.9	1.12
				2nd	0.927	91.4	96.0	66.9	1.10
				3rd	0.926	91.4	95.9	67.0	1.09
			120	1st	1.01	91.2	95.6	67.2	1.08
				2nd	1.00	91.1	94.2	67.1	1.06
				3rd	0.99	90.9	94.2	67.2	1.05
	150	56.7	80	1st	1.15	88.0	96.6	64.7	1.05
				2nd	1.14	88.0	96.4	64.7	1.05
				3rd	1.14	88.1	96.4	64.7	1.05
			120	1st	1.32	87.0	96.0	64.6	1.02
				2nd	1.31	87.0	95.8	64.5	1.01
				3rd	1.31	86.4	95.8	64.5	1.00
	190	55.4	80	1st	1.36	86.6	96.6	62.6	1.01
				2nd	1.34	86.6	96.6	62.6	1.01
				3rd	1.34	86.3	96.6	62.6	1.01

the three-cycles thermo–mechanical SM test. These experiments were performed at the programming temperature T_{pr} of 100 °C for EOC30 and 80 °C for EOC60 which are near to the finally melting temperature of these SCBPE.

In combination with Fig. 1, Fig. 2 demonstrates the strict correlations between the crystallinity and temperature dependence of the SM recovery strain $\varepsilon_{rec}(T)$ (Fig. 2a and c) and SM recovery rate $d\varepsilon_{rec}(T)/dt$ (Fig. 2 b and d) as well as between melting T_m and switching T_{sw} temperatures, respectively. The EOCs show a reduction of the T_{sw} value and SM recovery rate in the temperature range of melting and especially at the switching temperature $\lvert d\varepsilon_{rec}(T)/dt\rvert_{max}$ with decreasing melting temperature and crystallinity, respectively, due to the increase of both the degree of branching as a major influencing factor and the crosslink density ν_c (see Figs. 1 and 2 as well as Table 3). The shoulders in the $d\varepsilon_{rec}(T)/dt$ curves of EOC60 are caused by the existence of a thermodynamically less stable crystal population. The R_r values are approximately 95% and 96% for EOC30 and EOC60, respectively.

With increasing crosslink density ν_c of both EOCs a small increase of R_r of about 1% is observed. At the same time, R_f of EOC60 decreases considerably, whereas R_f of EOC30 increases only slightly with increasing ν_c value (see Fig. 2 and Table 3). In consequence of the increase of stresses occurred by programming (σ_{pr}) with constant strain of 100% and decrease of the ability of crystalline phase to fix these stresses due to the decrease of crystallinity and perfection of crystallites, R_f is generally expected to decrease with an increase of ν_c.

There is yet another difference in the SM behavior between EOC30 and EOC60. All highly branched EOC60 networks demonstrate a continuous decrease of $\varepsilon_{rec}(T)$ with increasing temperature. On the other hand, the medium branched EOC30 networks with ν_c values of 70 and 130 mol m^{-3} exhibit an increase of $\varepsilon_{rec}(T)$ values in the temperature range from 25 to 66 °C and 49 °C, respectively. Since these temperatures are consistent with the temperature of α-relaxation the described behavior can be explained by the contribution of α-relaxation, which is explicit evident only for slowly cooled low and medium branched SCBPEs [41]. This conclusion agrees well with the $\varepsilon_{rec}(T)$ behavior, which is demonstrated by high density PE for temperatures up to approximately 100 °C [43]. In highly branched EOC60 the temperature and intensity of α-relaxation is considerably lower and correspondingly the contribution of α-relaxation to SM recovery is insignificant [40].

Generally, the flatter and wider the melting endotherm the smaller and broader is the $\varepsilon_{rec}(T)$ peak of SMP (see Fig. 2). Thus, it can be concluded that the decrease of crystallinity and crystal perfection as well as the broadening of crystal size distribution, especially in direction of lower values, leads in any case to a deceleration of the SM recovery kinetics, even if the forces produced by programming increase as in the case of increasing crosslink density. This can be explained by an increment in difference between the elastic and viscoelastic forces produced by programming and stored/fixed in the specimen by crystallization due to an increase of a part of poorer and smaller crystallites in the entire spectrum.

For samples with a high degree of crosslinking the temperature dependencies of $\varepsilon_{rec}(T)$ and $d\varepsilon_{rec}(T)/dt$ obtained from the cyclic thermo–mechanical SM test at relatively low programming temperatures are practically congruent for all cycles (see Figs. 2 and 3a–d).

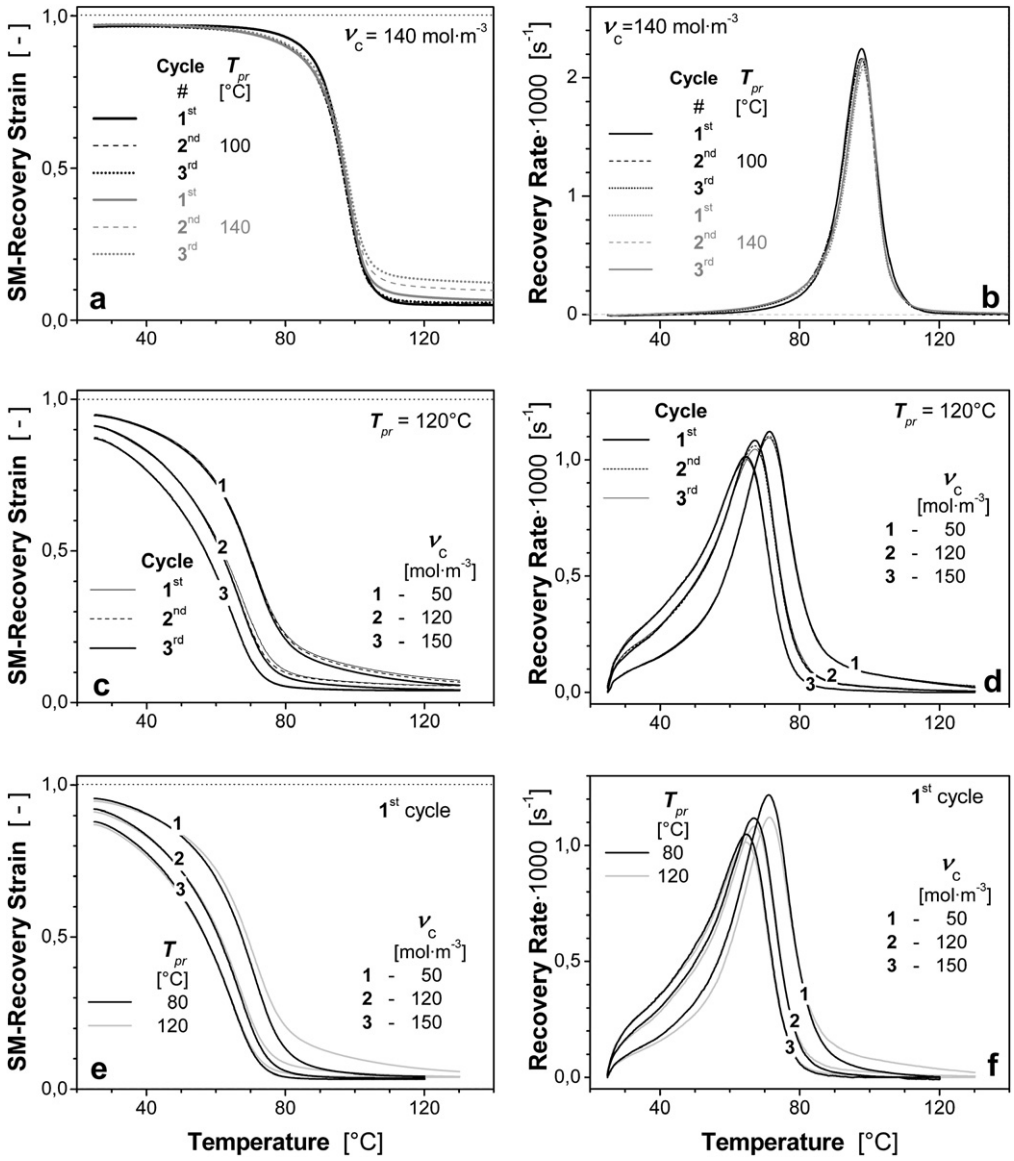

Fig. 3. Influence of programming temperature T_{pr} on dependencies of SM recovery strain (a, c, e) and recovery strain rate (b, d, f) measured for medium branched EOC30 (a, b) and highly branched EOC60 with different crosslink density ν_c (c–f).

Only the samples of EOC60 and EOC30 with lower degree of crosslinking of approximately 50 and 70 mol m^{-3} exhibit certain small differences between the curves detected in first, second or third cycle. In particular, such samples exhibit in the first cycle some lower $\varepsilon_{rec}(T)$ at $T > T_{sw}$ and correspondingly some higher R_r values as well as slightly higher values of $|d\varepsilon_{rec}(T)/dt|_{max}$. In any case, the differences between second and third cycle were generally negligible.

The situation changes appreciably, if T_{pr} becomes 40 K higher (see Fig. 3). At $T_{pr} = 140$ and 120 °C for EOC30 and EOC60, respectively, the reduction of R_r value in repeating cycles of SM test, as compared to 40 K lower T_{pr}, is evident. However, this behavior occurs more explicitly for specimens with ν_c values of approximately 50 to 140 mol m^{-3}. For EOC networks with higher ν_c values the influence of T_{pr} on the change of SM characteristics in cyclic thermo–mechanical test is not so distinct. In other respects the crosslinked EOCs show the similar SM behavior, as described above for 40 K lower T_{pr}. The optimal T_{pr} value must be chosen obviously between melting and crystallization temperatures, but in this case, the specimen should be pre-heated at a temperature higher than T_m before programming.

Table 3 demonstrates that the programming stress σ_{pr} gains with increasing programming temperature T_{pr} and crosslink density ν_c for both EOCs as expected according to the rubber elasticity theory. The medium branched EOC30 network produces markedly higher σ_{pr} values compared to highly branched EOC60 with similar crosslink density ν_c (140 and 150 mol m^{-3}, respectively) at the same T_{pr}. This difference can be explained by the abovementioned hypothesis discussed in Section 2.2, which assumes that the true local crosslink density of the amorphous phase is considerably higher as the experimentally obtained average values of crosslink density.

3.3. Effect of load during SM recovery of programmed EOC networks

The effect of load on SM recovery behavior of crosslinked EOC30 and EOC60 is demonstrated in Fig. 4. As previously discussed for unconstrained SM recovery, the SM recovery curves under load possess no significant change in the second and third SM cycles compared to the first cycle. The SME characteristics obtained in the first SM cycle are provided in Table 4. In this case, besides the R_f, R_r, T_{sw} and $|d\varepsilon_{rec}(T)/dt|_{max}$ values, it seems to be reasonable to use the

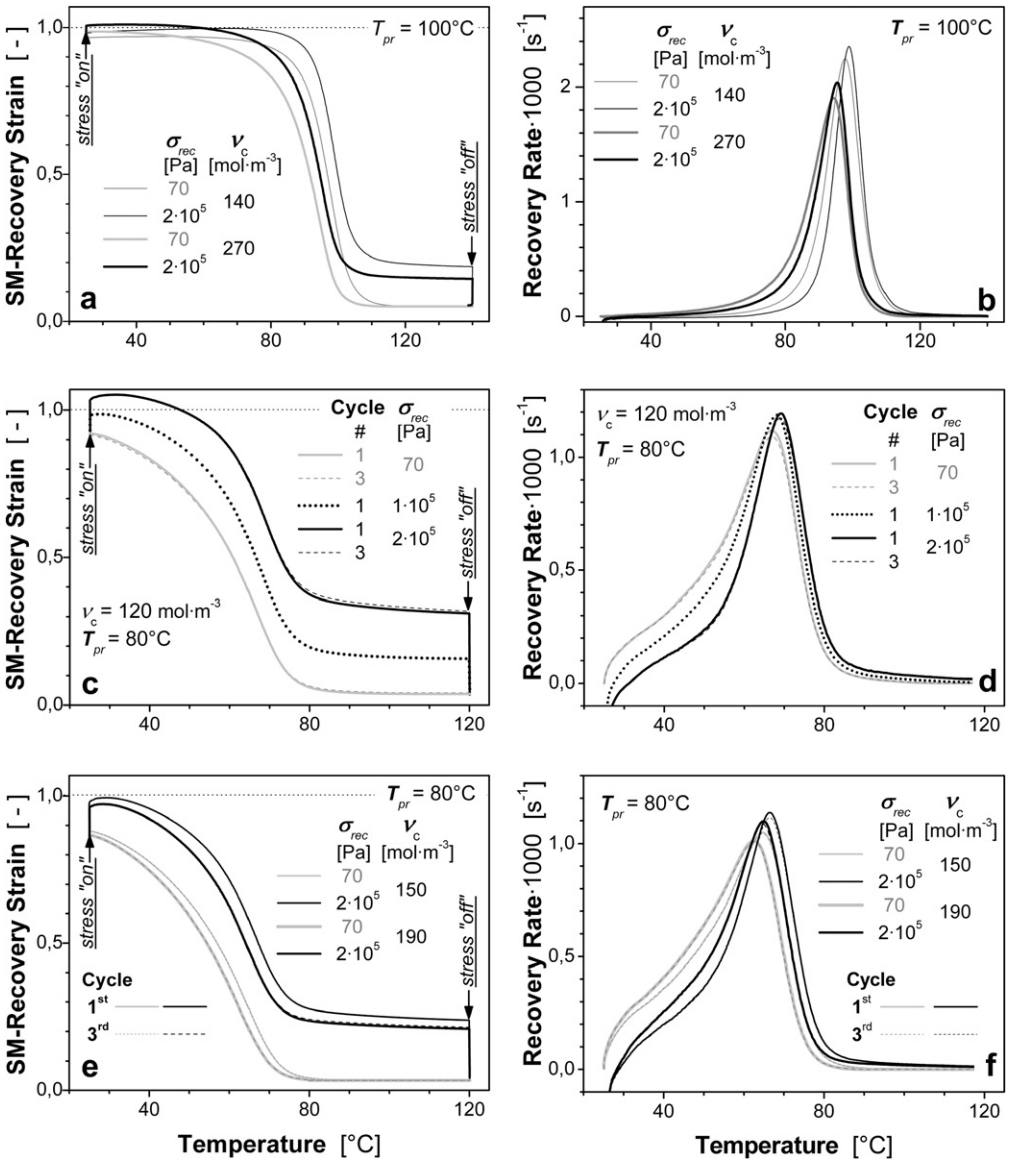

Fig. 4. Influence of load during SM recovery on dependencies of SM recovery strain (a, c, e) and SM recovery strain rate (b, d, f) measured at different σ_{rec} values (see legends) for EOC30 (a, b) and EOC60 (c–f) with different cross-link density ν_c after programming by 100% strain.

mechanical specific work W_{sp}, which is done by the elastic and viscoelastic forces stored in the volume unit of completely programmed specimen. The W_{sp} will be proposed for the characterization of SM recovery behavior under load with the external force, which opposes the clamp motion. At this point an important remark is to make that in presented experiments the nominal value of constraining stress σ_{rec} is related to the initial cross-section area of the sample before stretching.

Therefore, at programming strain of 100% used in the present work the true stress reduces in recovery run in the case of ideal SM behavior ($R_f = R_r = 100\%$) from $2\sigma_{rec}$ to σ_{rec} with increasing temperature, due to the increasing initial cross-section area of sample. In real case ($R_f < 100\%$ and $R_r < 100\%$) the true stress σ_{true} decreases in the range between $2\sigma_{rec} > \sigma_{true} > \sigma_{rec}$. By contrast, here the force was kept constant. For this reason, the specific work can be calculated as the product of maximum contraction of sample (at highest temperature of the experiment) and constant external opposed force per unit volume of sample.

In comparison to unconstrained recovery runs ($\sigma_{rec} = 70$ Pa) the SM recovery curves under load (here $\sigma_{rec} = 0.1$ or 0.2 MPa) are notably shifted upwards and evince distinctly lower R_r values as well as higher apparent R_f values, which can exceed 100%. Similar to the unconstrained recovery runs the temperature dependencies of recovery strain and recovery rate obtained under load σ_{rec} by cyclic thermo–mechanical SM test are nearly congruent, especially for samples with high crosslink density. The differences between first and third cycle were negligible.

For all investigated samples the peaks of SM recovery rate ascertained under load were shifted slightly to higher temperatures and evinced some higher $|d\varepsilon_{rec}(T)/dt|_{max}$ values compared to unconstrained recovery runs. The differences in switching temperatures and peak values of SM recovery rate between unconstrained recovery runs and recovery runs detected under load rise with increasing σ_{rec} value. However, these changes are relatively low (see Fig. 4 b, d and f as well as Table 4). Such a weak acceleration of the recovery kinetics could be connected with changed melting behavior of the samples under load.

With increasing crosslink density ν_c the programming stress σ_{pr} and obviously the stored elastic and viscoelastic forces increase markedly and correspondingly the recovery becomes more

Table 4
Influence of crosslink density ν_c and nominal value of constraining stress during SM recovery σ_{rec} on SME characteristics of medium and highly branched EOCs obtained in first SM cycle.

EOC type	T_{pr} [°C]	ν_c [mol m^{-3}]	σ_{rec} [Pa]	R_f [%]	R_r [%]	T_{sw} [°C]	$\lvert d\varepsilon_{rec}(T)/dt\rvert_{max}$ [10^{-3} s^{-1}]
EOC30	100	65	70	96.0	95.2	100.6	2.41
			2×10^5	97.0	64.7	102.0	2.52
		140	70	96.5	95.0	97.8	2.24
			2×10^5	99.3	81.4	99.0	2.36
		220	70	97.7	95.2	95.9	2.03
			2×10^5	99.7	85.2	97.0	2.17
		270	70	98.6	95.0	94.5	1.90
			2×10^5	100.3	85.4	95.5	2.04
EOC60	80	50	70	95.5	95.7	71.2	1.22
			1×10^5	100.9	73.0	72.5	1.29
		120	70	92.1	96.3	66.9	1.12
			1×10^5	98.3	84.3	68.2	1.19
			2×10^5	103.5	68.8	69.2	1.19
		150	70	88.0	96.6	64.7	1.05
			1×10^5	93.0	87.4	65.5	1.12
			2×10^5	98.0	76.1	66.5	1.14
		190	70	86.6	96.6	62.6	1.01
			1×10^5	90.8	88.7	63.8	1.08
			2×10^5	96.1	78.8	64.9	1.10

complete for both EOCs that results in a certain rise of strain recovery ratio R_r (see Fig. 4 a, c and e, Table 4 and Fig. 5). Fig. 5 demonstrates that the σ_{pr} value shows yet no linear dependence on ν_c, as expected according to the rubber elasticity theory. Regardless the rubber elasticity theory, the σ_{pr}, R_r and W_{sp} values exhibit a distinct tendency to the formation of a plateau with increasing ν_c. Thereby the W_{sp} value for highly branched EOC60 increases insignificantly. Allowing for the considerable increment of programming stress σ_{pr} with increasing crosslink density ν_c it can be concluded that there is only a weak qualitative correlation between the increase of σ_{pr} values and of specific work W_{sp} as well as of strain recovery ratio R_r. This observation points to the decrease of ability of crystalline phase to fix the forces generated in the network by programming with increasing crosslink density due to the abovementioned decrease of crystallinity and perfection of crystallites that results in an increase of the difference between programming stress and stored elastic/viscoelastic stress.

Two other peculiarities of SM recovery under load should be emphasized. Firstly, the W_{sp} value shows surprisingly a considerable rise with increasing external load, e.g., for EOC60 with

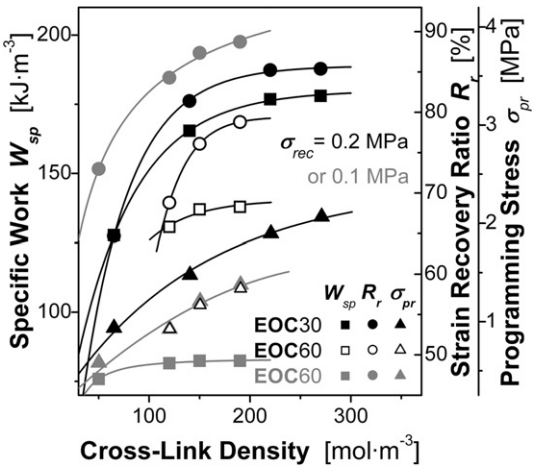

Fig. 5. Influence of cross-link density and degree of branching of EOCs on programming stress σ_{pr}, strain recovery ratio and R_r specific work W_{sp} done by SM recovery under load σ_{rec} of 0.2 MPa (black points and curves); the results obtained for EOC60 by σ_{rec} = 0.1 MPa are given in gray.

ν_c = 150 mol m^{-3} the W_{sp} value changes from 82 to 131 kJ m^{-3} as a result of σ_{rec} increase from 0.1 to 0.2 MPa. Secondly, the medium branched EOC30 produces a notably higher programming stress σ_{pr} and correspondingly realizes a considerably larger specific mechanical work W_{sp} compared to highly branched EOC60 with nearly the same crosslink density ν_c, e.g., EOC30 with ν_c = 140 mol m^{-3} and EOC60 with ν_c = 150 mol m^{-3} show the values σ_{pr} = 1.48 and 1.17 MPa as well as W_{sp} = 165 and 137 kJ m^{-3}, respectively. This means that the medium branched EOC30 in comparison to the highly branched EOC60 does not only produce a larger programming stress due to the higher programming/crystallization temperature and local crosslink density, but EOC is also able to fix the produced forces better as a consequence of higher crystallinity and crystal perfection.

4. Conclusions

Crystallinity, melting temperature and crosslinking density of crosslinked homogeneous ethylene-1-octene copolymers (EOCs) can be well controlled by the 1-octene content in the copolymer (degree of branching) and the amount of suitable peroxide, e.g., DHBP. Thus, short-chain branched polyethylenes (SCBPEs) can be applied as model shape memory (SM) polymers for the investigation of principles and mechanisms of the thermally-induced SM effect in covalently crosslinked semi-crystalline polymers.

The influence of crystallinity, melting temperature and crosslink density of semi-crystalline networks as well as of programming conditions, which include also the temperature-triggered changes of crystallinity on the kinetics and dynamics of the SM behavior of SCBPEs, has been analyzed. The findings of the investigation allow to make the following ascertainments, proposals and suggestions:

- The resulting switching temperature for all investigated crosslinked SCBPEs decreases systematically with increasing both the degree of branching and the crosslink density within the temperature range of 101 to 63 °C and shows a rather strict dependence on the melting temperature.
- In unconstrained SM recovery experiments the generated SCBPE networks exhibit high values of strain recovery ratio of about 97%, which increases only slightly with increasing crosslink density, in spite of simultaneous considerable rise of programming stress. The highly branched and correspondingly low crystalline SCBPE networks demonstrate a distinct decrease of strain fixity ratio with increasing crosslink density and programming stress. In contrast, the strain fixity ratio of medium crystalline SCBPE networks increase weakly with increasing crosslink density and programming stress as a result of the well developed crystalline structure and the markedly contribution of α relaxation to the SM recovery.
- The increase of branching degree and crosslink density results in the deceleration of the SM recovery kinetics, even though, the programming stress increase simultaneously. This is caused by the drop of ability of crystalline phase to fix the elastic/viscoelastic forces generated in the network due to the decrease of crystallinity, crystal size and perfection, and the broadening of crystal size distribution.
- Although, the elasticity modulus of covalent network and correspondingly the stress at constant strain increase with rising temperature, the stored stress, which will be fixed in the network by the crystalline structure, cannot exceed the lowest stress generated by the stretched network at crystallization temperature. Furthermore, the considerable increase of programming temperature causes a slight decrease of strain recovery and strain fixity ratios as well as of SM recovery rate, which can be explained by the acceleration of thermo-

oxidative degradation. Therefore, the optimal programming temperature must obviously be as low as possible and located in the window between melting and crystallization temperatures. In this case, the short-term heating above the melting temperature is necessary before programming.

- The mechanical specific work generated by the stored elastic/viscoelastic forces during SM recovery under load, which was calculated as the product of final contraction of sample and constant external opposed force per unit volume of the sample, can be used as dynamical SM characteristic of practical relevance. The investigation of constraining stress influence on the SM recovery behavior is very important for the estimation of application limits of given SM polymers. In comparison to unconstrained recovery runs, the SM recovery under load leads to distinctly lower strain recovery ratio but higher apparent strain fixity ratio, which can exceed 100%. The strain recovery ratio and mechanical specific work under load increase moderately with increasing crosslink density, in spite of simultaneous considerable increase of programming stress, that is especially evident for highly branched SCBPE. This points to distinct differences between the generated and stored stresses and to the strong effect of crystallinity and perfection of crystalline structure on the ability of SM polymer to store the generated forces.
- Compared to crosslinked conventional PEs, the crosslinked SCBPEs have a relatively low switching temperature, which can be tailored in the range between 60 and 100 °C by varying the degree of branching and crosslink density. Therefore, the results can serve for the development of innovative SM polymers and applications such polymers as heat-shrinkable molded items with reduced energy input. The results of the work contribute to a better understanding of the correlations between crystallization/relaxation processes, which are behind the SM effect, and the parameters of the SM behavior, necessary for process optimization.

Acknowledgment

The authors gratefully acknowledge the financial support by Deutsche Forschungsgemeinschaft (DFG). Samples of DHBP peroxide were kindly provided by Evonic Degussa GmbH (Germany).

References

[1] Lendlein A, Kelch S. Angew Chem Int Ed 2002;41:2034–57.
[2] Behl M, Lendlein A. Soft Mater 2007;3:58–67.
[3] Liu C, Qin H, Mather PT. J Mater Chem 2007;17:1543–58.
[4] Ratna D, Karger-Kocsis J. J Mater Sci 2008;43:254–69.
[5] Hornbogen E. Adv Eng Mater 2006;8(1–2):101–6.
[6] Beloshenko VA, Varyukhin VN, Voznyak YV. Usp Khim 2005;74(3):285–306.
[7] Ota S. Radiat Phys Chem 1981;18:81–7.
[8] Kleinheins G, Starkl W, Nuffer K. Kunststoffe 1984;74:445–9.
[9] Lendlein A, Langer R. Science 2002;296:1673–6.
[10] Lee AP, Northrup MA, Ciarlo DR, Krulevitch PA, Benett WJ. US patent 6102933; 2000.
[11] Bellin I, Kelch S, Langer R, Lendlein A. Proc Natl Acad Sci USA 2006;103: 18043–7.
[12] Lendlein A, Kelch S. Clin Hemorheol Microcirc 2005;32:105–16.
[13] Small W, Wilson TS, Benett WJ, Loge JM, Maitland DJ. Opt Express 2005;13(20):8204–13.
[14] Baer GM, Small W, Wilson TS, Benett TJ, Matthews DL, Hartman J, et al. BioMedical Eng OnLine 2007;6:43.
[15] Tobushi H, Hayashi S, Kojima S. JSME Int J Ser 1 1992;35:296–302.
[16] Takahashi T, Hayashi N, Hayashi S. J Appl Polym Sci 1996;60(7):1061–9.
[17] Choi NY, Kelch S, Lendlein A. Adv Eng Mat 2006;8(5):439–45.
[18] Lendlein A, Schmidt AM, Langer R. Proc Natl Acad Sci USA 2001;98(3):842–7.
[19] Choi NY, Lendlein A. Soft Matter 2007;3(7):901–9.
[20] Alteheld A, Feng Y, Kelch S, Lendlein A. Angew Chem Int Ed 2005;44(8): 1188–92.
[21] Li F, Chen Y, Zhu W, Zhang X, Xu M. Polymer 1998;39:6929–34.
[22] Li F, Zhu W, Zhang X, Zhao C, Xu M. J Appl Polym Sci 1999;71:1063–70.
[23] Gall K, Dunn ML, Liu Y, Finch D, Lake M, Munshi NA. Acta Mater 2002;50: 5115–26.
[24] Liu Y, Gall K, Dunn ML, McCluskey P. Smart Mater Struct 2003;12:947–54.
[25] Liu Y, Gall K, Dunn ML, McCluskey P. Mech Mater 2004;36:929–40.
[26] Liu Y, Gall K, Dunn ML, Greenberg AR, Diani J. Int J Plasticity 2006;22:279–313.
[27] Diani J, Liu Y, Gall K. Polym Eng Sci 2006;46:486–92.
[28] Liu Ch, Chun SB, Mather PT, Zheng L, Haley EH, Coughlin EB. Macromolecules 2002;35:9868–74.
[29] Bensason S, Minick J, Moet A, Chum S, Hiltner A, Baer E. J Polym Sci B Polym Phys 1996;34:1301–15.
[30] Loan LD. J Polym Sci A 1964;2:3053–66.
[31] Lal J, McGrath JE, Board RD. J Polym Sci A 1 1968;6:821–8.
[32] Harpell GA, Walrod DH. Rubber Chem Technol 1973;46:1007–18.
[33] Sajkiewicz P, Phillips PJ. J Polym Sci A 1995;33:853–62.
[34] Loan LD. Pure Appl Chem 1972;30:173–80.
[35] Flory PJ, Rehner J. J Chem Phys 1943;11:512–20, 521–6.
[36] Smedberg A, Hjertberg T, Gustafsson B. Polymer 2003;44:3395–405.
[37] Hoffmann M. Kolloid Z Z Polym 1972;250:197–206.
[38] Heinrich G, Straube E, Helmis G. Acta Polym 1980;31:275–86.
[39] Kolesov IS, Androsch R, Radusch H-J. J Therm Anal Cal 2004;78:885–95.
[40] Kolesov IS, Androsch R, Radusch H- J. Macromolecules 2005;38:445–53.
[41] Mathot VBF, Scherrenberg RL, Pijpers MFJ, Bras W. J Therm Anal 1996;46: 681–718.
[42] Androsch R, Wunderlich B. Macromolecules 1999;32:7238–46.
[43] Kolesov IS, Radusch H-J. eXPRESS Polym Lett 2008;2:461–73.